Identification of two dimensional complex sinusoids in white noise: a state–space frequency approach

Umberto Soverini * **Torsten Söderström** **

* *Department of Electrical, Electronic and Information Engineering, University of Bologna, Italy (e-mail: umberto.soverini@unibo.it)*
** *Department of Information Technology, Uppsala University, Sweden (e-mail: ts@it.uu.se)*

Abstract: This paper proposes a new frequency domain approach for identifying the parameters of two–dimensional complex sinusoids from a finite number of data, when the measurements are affected by additive and uncorrelated two–dimensional white noise. The new method extends in two dimensions a frequency identification procedure of complex sinusoids, originally developed for the one–dimensional case. The properties of the proposed method are analyzed by means of Monte Carlo simulations and its features are compared with those of other estimation algorithms. In particular the practical advantage of the method is highlighted. In fact the novel approach can operate just on a specified sub–area of the 2D spectrum. This area–selective feature allows a drastic reduction of the computational complexity, which is usually very high when standard time domain methods are used.

Keywords: System identification; Discrete Fourier Transform; 2D damped sinusoidal models.

1. INTRODUCTION

In many engineering applications, such as image processing and Magnetic Resonance (MR) spectroscopy, high–resolution methods are used to determine with accuracy the parameters of two–dimensional (2D) signals.

Among these methods, one can find the harmonic retrieval method (Kung et al., 1983), the MEMP method (Hua, 1992; Hua and Baqai, 1994; Zhu and Hua, 1993) and the ACMP method (Vanpoucke et al., 1994). Other approaches are the 2D–Prony method (Sacchini et al., 1993), the Linear Prediction method, see e.g. (Marple, 2000), the 2D-MODE algorithm (Li et al., 1996), the 2D–MUSIC method (Li et al., 1998) and the 2D–ESPRIT method (Rouquette and Najim, 2001; Wang et al., 2005).

Many of these methods have been originally proposed for estimating the frequency parameters of one–dimensional (1D) signals (Stoica and Moses, 1997), and successively they have been extended to the 2D case. As a common distinguishing property, all these methods share the fact that the data are treated in the time domain.

In recent years the theoretical results provided by (Pintelon et al., 1997), with reference to input–output models, and by (McKelvey, 2000, 2002), for state–space models, have allowed to directly implement in the frequency domain many 1D parametric approaches originally developed for time domain data (Pintelon and Schoukens, 2012).

Based on these results, in (Soverini and Söderström, 2017) a new frequency subspace–based approach has been proposed for the identification of noisy complex sinusoids and in (Soverini and Söderström, 2018) the same approach has been extended to the 2D case. Following the idea of (Pintelon et al., 1997), these papers solve the harmonic retrieval problem by using input–output representations.

In this paper, the problem of identifying the parameters of 2D complex sinusoids from noisy measurements is based on a state–space frequency domain approach. Similarly to (McKelvey and Viberg, 2001), also in this case the solution is obtained by reformulating the original problem into a new one, where the original data become N–periodic. As a major feature, the method enables the estimation to be frequency area–selective, i.e. the user has the possibility to take into account some *a priori* information and select the data just from the 2D frequency sub–bands in which the signal harmonics are known to reside.

The organization of the paper is as follows. Section 2 defines the problem of identifying 2D complex sinusoids buried in white measurement noise. Section 3 introduces a novel frequency domain state–space representation of the 2D system model. Section 4 describes the new frequency domain subspace–based algorithm, that will be denoted as 2D–F–ESPRIT method since it can be considered as the extension to the 2D case of the F–ESPRIT method, originated by the work of (McKelvey and Viberg, 2001), see e.g. (Gunnarsson and McKelvey, 2007). In Section 5 the effectiveness of the proposed method is verified by means of Monte Carlo simulations. In particular, the new method is compared with the 2D time domain method of (Kung et al., 1983) and the 2D–FD–ESPRIT–ENH method, recently proposed in (Soverini and Söderström, 2018). It is shown that 2D–F–ESPRIT and the 2D–FD–ESPRIT–ENH methods have very similar behaviors and are both characterized by high frequency resolution properties. Finally, some concluding remarks are reported in Section 6.

2. STATEMENT OF THE PROBLEM

Consider the following discrete time model for n 2D complex sinusoids buried in measurement noise

$$x(t_1,t_2)=\sum_{i=1}^{n}\rho_i\,\mathrm{e}^{\gamma_{1i}\,t_1}\,\mathrm{e}^{\gamma_{2i}\,t_2} \tag{1}$$

$$y(t_1,t_2)=x(t_1,t_2)+v(t_1,t_2), \tag{2}$$

where $t_1=0,\ldots,N_1-1$, $t_2=0,\ldots,N_2-1$ and N_1, N_2 denote the number of the available samples in each of the two dimensions.

The coefficients $\gamma_{1i}=-\beta_{1i}+\mathrm{i}\omega_{1i}$ and $\gamma_{2i}=-\beta_{2i}+\mathrm{i}\omega_{2i}$ contain the unknown damping and frequency parameters, $\rho_i=|\rho_i|\mathrm{e}^{\mathrm{i}\varphi_i}$ are the unknown complex gains and $v(t_1,t_2)$ is the complex 2D white noise.

The problem under consideration is to estimate the signal parameters ω_{1i}, β_{1i}, ω_{2i}, β_{2i} $(i=1,\ldots,n)$ and, possibly, the noise variance σ_v^*.

The following assumptions are applied.

A1. The number n is *a priori* known and all the components are present, $\rho_i\neq 0\ \forall i$.

A2. The n frequencies are distinct in both directions, i.e. $\omega_{1h}\neq\omega_{1l}$ and $\omega_{2h}\neq\omega_{2l}\ \forall h,l\ h\neq l$, with $\omega_{1h},\omega_{2h}\in(-\pi,\pi]$.

A3. The additive noise $v(t_1,t_2)$ is a 2D, zero–mean, complex–valued circular white noise, with *unknown* variance σ_v^* and is uncorrelated with $x(t_1,t_2)$.

The complex signals $x(t_1,t_2)$, $y(t_1,t_2)$ defined in (1)–(2) can be represented with the following separable 2D state-space model, see (Kung et al., 1983)

$$z(t_1+1,t_2)=F_1\,z(t_1,t_2)\qquad z(0,0)=z_0 \tag{3}$$

$$z(t_1,t_2+1)=F_2\,z(t_1,t_2) \tag{4}$$

$$x(t_1,t_2)=H\,z(t_1,t_2) \tag{5}$$

$$y(t_1,t_2)=x(t_1,t_2)+v(t_1,t_2), \tag{6}$$

where

$$F_1=\mathrm{diag}\,[\,\lambda_{11},\,\lambda_{12},\ldots,\lambda_{1n}\,] \tag{7}$$

$$F_2=\mathrm{diag}\,[\,\lambda_{21},\,\lambda_{22},\ldots,\lambda_{2n}\,] \tag{8}$$

$$H=[\underbrace{1,\,1,\ldots,1}_{n}] \tag{9}$$

$$z_0=[\,\rho_1,\,\rho_2,\ldots,\rho_n\,]^T \tag{10}$$

and

$$\lambda_{1i}=\mathrm{e}^{\gamma_{1i}}\qquad\lambda_{2i}=\mathrm{e}^{\gamma_{2i}}\qquad i=1,\ldots,n. \tag{11}$$

Note that for the exact definition of (3)–(5) for all time arguments, proper initial conditions $z(0,0)=z_0$ must be set.

The system (3)–(5) is a special case of the Roesser's model (Roesser, 1975)

$$r(t_1+1,t_2)=A_{11}\,r(t_1,t_2)+A_{12}s(t_1,t_2) \tag{12}$$

$$s(t_1,t_2+1)=A_{21}\,r(t_1,t_2)+A_{22}s(t_1,t_2) \tag{13}$$

$$w(t_1,t_2)=C_1\,r(t_1,t_2)+C_2\,s(t_1,t_2) \tag{14}$$

where

$$r(t_1,t_2)=s(t_1,t_2)=z(t_1,t_2) \tag{15}$$

$$w(t_1,t_2)=x(t_1,t_2) \tag{16}$$

and

$$A_{11}=F_1\quad A_{22}=F_2\quad A_{12}=A_{21}=0 \tag{17}$$

$$C_1=C_2=\frac{1}{2}H. \tag{18}$$

In this paper the identification problem is faced in the frequency domain, using the Discrete Fourier Transform (DFT) of the signals. In (Soverini and Söderström, 2018) the problem was treated in the frequency domain using an input–output representation. In this paper the problem is instead formulated using state space techniques and an exact description of the effects of the initial conditions is given and exploited.

As a main feature, the estimation procedure can work using only a subset of the 2D–frequency domain, that is part of the ω_1,ω_2 space.

For a generic 1D signal $\{s(t)\}_{t=0}^{N-1}$, observed at N equidistant time instants, the one–dimensional Discrete Fourier Transform (1D–DFT) is defined as

$$S(\omega_h)=\frac{1}{\sqrt{N}}\sum_{t=0}^{N-1}s(t)\,\mathrm{e}^{-\mathrm{i}\omega_h t}, \tag{19}$$

where $\omega_h=2\pi h/N$, $h=0,\ldots,N-1$.

For a generic 2D signal $s(t_1,t_2)$ with $t_1=0,\ldots,N_1-1$, $t_2=0,\ldots,N_2-1$, observed at equidistant time instants, the two–dimensional Discrete Fourier Transform (2D–DFT) is defined as

$$S(\omega_h,\omega_l)=\frac{1}{\sqrt{N_1N_2}}\sum_{t_1=0}^{N_1-1}\sum_{t_2=0}^{N_2-1}s(t_1,t_2)\,\mathrm{e}^{-\mathrm{i}\omega_h t_1}\,\mathrm{e}^{-\mathrm{i}\omega_l t_2} \tag{20}$$

where $\omega_h=2\pi h/N_1$ $(h=0,\ldots,N_1-1)$ and $\omega_l=2\pi l/N_2$ $(l=0,\ldots,N_2-1)$.

By using the definition (19), the 2D–DFT (20) can be obtained in two steps, by computing the DFT with respect to t_1, keeping t_2 fixed

$$\bar{S}_1(\omega_h,t_2)=\frac{1}{\sqrt{N_1}}\sum_{t_1=0}^{N_1-1}s(t_1,t_2)\,\mathrm{e}^{-\mathrm{i}\omega_h t_1} \tag{21}$$

and next computing the DFT of $\bar{S}_1(\omega_h,t_2)$ with respect to t_2

$$S(\omega_h,\omega_l)=\frac{1}{\sqrt{N_2}}\sum_{t_2=0}^{N_2-1}\bar{S}_1(\omega_h,t_2)\,\mathrm{e}^{-\mathrm{i}\omega_l t_2}. \tag{22}$$

Or *vice versa*, one can firstly proceed with respect to t_2 and then with respect to t_1

$$\bar{S}_2(t_1,\omega_l)=\frac{1}{\sqrt{N_2}}\sum_{t_2=0}^{N_2-1}s(t_1,t_2)\,\mathrm{e}^{-\mathrm{i}\omega_l t_2} \tag{23}$$

$$S(\omega_h,\omega_l)=\frac{1}{\sqrt{N_1}}\sum_{t_1=0}^{N_1-1}\bar{S}_2(t_1,\omega_l)\,\mathrm{e}^{-\mathrm{i}\omega_h t_1}. \tag{24}$$

It is worth observing that the 1D–DFT in (19) and the 2D–DFT in (20) can be expressed also in matrix form, see Appendix A of (Soverini and Söderström, 2018).

The problem under investigation can be stated as follows.

Problem 1. Let $Y(\omega_h,\omega_l)$ $(h=0,\ldots,N_1-1;\ l=0,\ldots,N_2-1)$ be the 2D–DFT of the noisy measurements $y(t_1,t_2)$ generated by the system (1)–(2). Given $Y(\omega_h,\omega_l)$, estimate the signal parameters ω_{1i}, β_{1i}, ω_{2i}, $\beta_{2i}(i=1,\ldots,n)$.

Remark 1. The main focus is on the non–linear problem of estimating the parameters $\gamma_{1i}=-\beta_{1i}+\mathrm{i}\omega_{1i}$ and $\gamma_{2i}=-\beta_{2i}+\mathrm{i}\omega_{2i}$. Once the parameters γ_{1i} and γ_{2i} are known, in order to recover the model (1) it is necessary to develop a

further procedure for pairing them properly $\{\gamma_{1i}, \gamma_{2i}\}_{i=1}^{n}$ and for estimating the parameters ρ_i. For example, one can apply the procedure described in (Sandgren et al., 2006), which is briefly recalled in Appendix B. The estimation of σ_v^* remains as the final step, not pursued here. $\diamond$

3. FREQUENCY DOMAIN STATE SPACE REPRESENTATION

In the following, it is developed a 2D state–space representation that is the frequency counterpart of the time domain model (3)–(5).

With reference to the state vector $z(t_1, t_2)$ and the output signal $x(t_1, t_2)$, let $\bar{Z}_1(\omega_h, t_2)$ and $\bar{X}_1(\omega_h, t_2)$ be the 1D–DFTs with respect to t_1, see (21). In an analogous way, let $\bar{Z}_2(t_1, \omega_l)$ and $\bar{X}_2(t_1, \omega_l)$ be the 1D–DFTs with respect to t_2, see (23).

By introducing the terms $W_{N_1} = \mathrm{e}^{\mathrm{i}\frac{2\pi}{N_1}}$ and $W_{N_2} = \mathrm{e}^{\mathrm{i}\frac{2\pi}{N_2}}$ and recalling the results of (McKelvey and Viberg, 2001), the following 1D–DFT of the state–space model (3)–(5) can be obtained

$$W_{N_1}^h \, \bar{Z}_1(\omega_h, t_2) = F_1 \, \bar{Z}_1(\omega_h, t_2) + \frac{T_1(t_2)}{\sqrt{N_1}} \, W_{N_1}^h \tag{25}$$

$$W_{N_2}^l \, \bar{Z}_2(t_1, \omega_l) = F_2 \, \bar{Z}_2(t_1, \omega_l) + \frac{T_2(t_1)}{\sqrt{N_2}} \, W_{N_2}^l \tag{26}$$

$$\bar{X}_1(\omega_h, t_2) = H \, \bar{Z}_1(\omega_h, t_2) \tag{27}$$

$$\bar{X}_2(t_1, \omega_l) = H \, \bar{Z}_2(t_1, \omega_l). \tag{28}$$

Remark 2. The vector $T_1(t_2) = z(0, t_2) - z(N_1, t_2)$ represents the transient term due to the difference between the initial state $z(0, t_2)$ and the final state $z(N_1, t_2) = F_1^{N_1} \, z(0, t_2)$. It must be observed that the vector T_1 is an explicit function of t_2, since changing t_2 the values of its entries change. In an analogous way, the vector $T_2(t_1) = z(t_1, 0) - z(t_1, N_2)$ represents the transient term due to the difference between the initial state $z(t_1, 0)$ and the final state $z(t_1, N_2) = F_2^{N_2} \, z(t_1, 0)$. $\diamond$

According to (20), let $X(\omega_h, \omega_l)$, $Z(\omega_h, \omega_l)$, $V(\omega_h, \omega_l)$ and $Y(\omega_h, \omega_l)$ be the 2D–DFTs of the time domain sequences $x(t_1, t_2)$, $z(t_1, t_2)$, $v(t_1, t_2)$ and $y(t_1, t_2)$, respectively.

Compute now the 1D–DFT on both sides of relation (25) with respect to t_2. It results in

$$W_{N_1}^h \, Z(\omega_h, \omega_l) = F_1 \, Z(\omega_h, \omega_l) + \frac{\bar{T}_1(\omega_l)}{\sqrt{N_1}} \, W_{N_1}^h, \tag{29}$$

where $\bar{T}_1(\omega_l)$ is the 1D–DFT of the sequence $T_1(t_2)$

$$\bar{T}_1(\omega_l) = \frac{1}{\sqrt{N_2}} \sum_{t_2=0}^{N_2-1} T_1(t_2) \, \mathrm{e}^{-\mathrm{i}\omega_l t_2}. \tag{30}$$

In a similar way, compute the 1D–DFT on both sides of relation (26) with respect to t_1. It results in

$$W_{N_2}^l \, Z(\omega_h, \omega_l) = F_2 \, Z(\omega_h, \omega_l) + \frac{\bar{T}_2(\omega_h)}{\sqrt{N_2}} \, W_{N_2}^l, \tag{31}$$

where $\bar{T}_2(\omega_h)$ is the 1D–DFT of the sequence $T_2(t_1)$

$$\bar{T}_2(\omega_h) = \frac{1}{\sqrt{N_1}} \sum_{t_1=0}^{N_1-1} T_2(t_1) \, \mathrm{e}^{-\mathrm{i}\omega_h t_1}. \tag{32}$$

Summing up, the previous results can be formalized in the following theorem.

Theorem 1. Let $X(\omega_h, \omega_l)$ be the 2D–DFT of the signal $x(t_1, t_2)$, generated by the 2D model (1), with finite values of N_1 and N_2. The following 2D–DFT representation for the state–space model (3)–(6) holds

$$W_{N_1}^h \, Z(\omega_h, \omega_l) = F_1 \, Z(\omega_h, \omega_l) + \frac{\bar{T}_1(\omega_l)}{\sqrt{N_1}} \, W_{N_1}^h \tag{33}$$

$$W_{N_2}^l \, Z(\omega_h, \omega_l) = F_2 \, Z(\omega_h, \omega_l) + \frac{\bar{T}_2(\omega_h)}{\sqrt{N_2}} \, W_{N_2}^l \tag{34}$$

$$X(\omega_h, \omega_l) = H \, Z(\omega_h, \omega_l) \tag{35}$$

$$Y(\omega_h, \omega_l) = X(\omega_h, \omega_l) + V(\omega_h, \omega_l), \tag{36}$$

where $\bar{T}_1(\omega_l)$ and $\bar{T}_2(\omega_h)$ are the vectors defined in (30) and (32), respectively. The term $\bar{T}_1(\omega_l)$ is null if $X(\omega_h, \omega_l)$ is N_1–periodic with respect to ω_h. Analogously, the term $\bar{T}_2(\omega_h)$ is null if $X(\omega_h, \omega_l)$ is N_2–periodic with respect to ω_l. $\diamond$

4. A FREQUENCY SUBSPACE–BASED METHOD

In this section a new 2D–frequency domain identification procedure is proposed. The procedure is the extension to the 2D case of the F–ESPRIT method, originated by the work of (McKelvey and Viberg, 2001). For this reason it will be denoted as 2D–F–ESPRIT algorithm.

The procedure shows also some common aspects with the 2D time domain realization procedure described in (Kung et al., 1983), denoted in the following as the 2D–TD–KUNG method. A revised version of the latter is briefly recalled in Appendix A.

Consider the state space equations (33) and (35), referring to the state transition matrix F_1. For every fixed value of ω_l, e.g. $\omega_l = \bar{\omega}_l$, the vector $\bar{T}_1(\bar{\omega}_l)$ is constant. The equations

$$W_{N_1}^h \, Z(\omega_h, \bar{\omega}_l) = F_1 \, Z(\omega_h, \bar{\omega}_l) + \frac{\bar{T}_1(\bar{\omega}_l)}{\sqrt{N_1}} \, W_{N_1}^h \tag{37}$$

$$X(\omega_h, \bar{\omega}_l) = H \, Z(\omega_h, \bar{\omega}_l) \tag{38}$$

represent a 1D state–space model that exactly coincide with equations (47)–(48) in (Soverini and Söderström, 2017) when the following substitutions are introduced

$$k = h \qquad N = N_1 \qquad A = F_1 \qquad C = H$$

$$Z(\omega_k) = Z(\omega_h, \bar{\omega}_l) \quad X(\omega_k) = X(\omega_h, \bar{\omega}_l) \quad T = \bar{T}_1(\bar{\omega}_l).$$

The notations in (37)–(38) can be further simplified, by denoting $Z_h = Z(\omega_h, \bar{\omega}_l)$, $X_h = X(\omega_h, \bar{\omega}_l)$ and $B_1 = \bar{T}_1(\bar{\omega}_l)/\sqrt{N_1}$. The resulting model

$$W_{N_1}^h \, Z_h = F_1 \, Z_h + B_1 \, W_{N_1}^h \tag{39}$$

$$X_h = H \, Z_h \tag{40}$$

is directly comparable with the one used in (Gunnarsson and McKelvey, 2007) and the references therein.

The F–ESPRIT algorithm is presented here with reference to the noise free data. The study of the noisy case requires a deeper analysis, not pursued here. Reasoning by columns, with reference to the generic l–th column of the 2D–DFT matrix $\mathbf{X}$ ($0 \leq l \leq N_2 - 1$), the main steps of the procedure are the following.

Select an integer $m > n$ (a user choice) and construct a vector relation by repeatedly using (39). For $h = 0, \ldots, N_1 - 1$, it results in

$$\bar{\mathbf{X}}_h = \mathcal{O}_{(m+1)} \, Z_h + \mathbf{\Gamma}_{(m+1)} \mathbf{U}_h \tag{41}$$

where

$$\bar{\mathbf{X}}_h = \begin{bmatrix} X_h \\ W_{N_1}^h X_h \\ W_{N_1}^{2h} X_h \\ \vdots \\ W_{N_1}^{mh} X_h \end{bmatrix} \qquad \mathbf{U}_h = \begin{bmatrix} W_{N_1}^h \\ W_{N_1}^{2h} \\ W_{N_1}^{3h} \\ \vdots \\ W_{N_1}^{(m+1)h} \end{bmatrix} \tag{42}$$

$$\mathcal{O}_{(m+1)} = \begin{bmatrix} H \\ HF_1 \\ HF_1^2 \\ \vdots \\ HF_1^m \end{bmatrix} \tag{43}$$

and

$$\mathbf{\Gamma}_{(m+1)} = \begin{bmatrix} 0 & 0 & \dots & 0 & 0 \\ HB_1 & 0 & \dots & 0 & 0 \\ HF_1B_1 & H\,B_1 & \dots & 0 & 0 \\ \vdots & \vdots & \ddots & \vdots & \vdots \\ HF_1^{(m-1)}B_1 & HF_1^{(m-2)}B_1 & \dots & HB_1 & 0 \end{bmatrix} \tag{44}$$

The value of m has been chosen here congruently with the algorithms proposed in the previous papers, see e.g. the considerations about equation (A.17) in Appendix A.

Defining the data matrices

$$\bar{\mathbf{X}} = \left[\bar{\mathbf{X}}_0 \;\; \bar{\mathbf{X}}_1 \;\; \dots \;\; \bar{\mathbf{X}}_{N_1-1}\right] \tag{45}$$

$$\mathbf{Z} = \left[Z_0 \;\; Z_1 \;\; \dots \;\; Z_{N_1-1}\right] \tag{46}$$

$$\mathbf{U} = \left[\mathbf{U}_0 \;\; \mathbf{U}_1 \;\; \dots \;\; \mathbf{U}_{N_1-1}\right], \tag{47}$$

the signal model can be written as follows

$$\bar{\mathbf{X}} = \mathcal{O}_{(m+1)}\mathbf{Z} + \mathbf{\Gamma}_{(m+1)}\mathbf{U}. \tag{48}$$

The structure of equation (48) is common to many subspace identification methods. The second term in (48) can be removed by a multiplication from the right by the following projection matrix

$$\mathbf{\Pi}^{\perp} = \mathbf{I} - \mathbf{U}^*(\mathbf{U}\mathbf{U}^*)^{-1}\mathbf{U}. \tag{49}$$

The resulting equation is

$$\bar{\mathbf{X}}\mathbf{\Pi}^{\perp} = \mathcal{O}_{(m+1)}\mathbf{Z}\mathbf{\Pi}^{\perp}. \tag{50}$$

In (50) the observability matrix $\mathcal{O}_{(m+1)}$ carries information about F_1. It can be extracted from the range space of the left hand side in (50). One can proceed by computing the $(m+1)\times(m+1)$ matrix

$$\begin{aligned} \mathbf{\Sigma}_l &= \bar{\mathbf{X}}\mathbf{\Pi}^{\perp}\left(\bar{\mathbf{X}}\mathbf{\Pi}^{\perp}\right)^H \\ &= \mathcal{O}_{(m+1)}\mathbf{Z}\mathbf{\Pi}^{\perp}(\mathbf{Z}\mathbf{\Pi}^{\perp})^H\mathcal{O}_{(m+1)}^H \\ &= \mathcal{O}_{(m+1)}\,\mathbf{P}_l\,\mathcal{O}_{(m+1)}^H \end{aligned} \tag{51}$$

where

$$\mathbf{P}_l = \mathbf{Z}\mathbf{\Pi}^{\perp}(\mathbf{\Pi}^{\perp})^H\mathbf{Z}^H. \tag{52}$$

The index l in $\mathbf{\Sigma}_l$ and $\mathbf{P}_l$ has been introduced for recalling that the previous procedure refers only to the l–th column of $\mathbf{X}$. Repeating the procedure for all the N_2 columns of $\mathbf{X}$ and averaging over all matrices $\mathbf{\Sigma}_l$ and $\mathbf{P}_l$, with $l \in [0, N_2-1]$, the final expression results in

$$\mathbf{\Sigma} = \mathcal{O}_{(m+1)}\,\mathbf{P}\,\mathcal{O}_{(m+1)}^H. \tag{53}$$

The matrix $\mathcal{O}_{(m+1)}$ in (53) appears also in (A.3) of the Appendix A, with the notation $\mathcal{O}_1$. Utilizing its particular structure, it is possible to compute the state–transition matrix F_1 using the shift–invariance property described by the relations (A.11)–(A.13). The signal parameters are then recovered from the eigenvalues of F_1.

Table 1. System parameters

	ω_{1i}	ω_{2i}	β_{1i}	β_{2i}	ρ_i
$i=1$	0.200	−0.010	0.06	0.06	$70\,\mathrm{e}^{0.5\pi}$
$i=2$	−0.225	0.185	0.07	0.08	$100\,\mathrm{e}^{0.5\pi}$
$i=3$	−0.210	0.200	0.07	0.09	$100\,\mathrm{e}^{0.5\pi}$
$i=4$	0.050	−0.060	0.13	0.09	$120\,\mathrm{e}^{0.5\pi}$
$i=5$	0.060	0.320	0.21	0.29	$400\,\mathrm{e}^{0.5\pi}$

By computing the eigenvalue decomposition

$$\mathbf{\Sigma} = U\,\mathbf{\Lambda}\,U^H, \tag{54}$$

the classical ESPRIT algorithm can be applied, see also Section 5 in (Soverini and Söderström, 2017).

Remark 3. It is worth observing that, for numerical robustness against rounding errors, it is preferable to proceed by computing the singular value decomposition of matrices of type $\bar{\mathbf{X}}\mathbf{\Pi}^{\perp}$, as defined in (50), instead of squaring them as proposed in (51) and computing the eigenvalue decomposition as suggested in (54). Indeed, this is the usual procedure followed for example in (Gunnarsson and McKelvey, 2007). However, the procedure described here has been preferred for the sake of clarity in the exposition and uniformity with the notations used for the algorithms presented in (Soverini and Söderström, 2017).

Analogous considerations hold for the equations (34) and (35) with reference to F_2. In this case, for every fixed value of ω_h, e.g. $\omega_h = \bar{\omega}_h$, the vector $\bar{T}_2(\bar{\omega}_h)$ is constant. The equations

$$W_{N_2}^l\,Z(\bar{\omega}_h,\omega_l) = F_2\,Z(\bar{\omega}_h,\omega_l) + \frac{\bar{T}_2(\bar{\omega}_h)}{\sqrt{N_2}}\,W_{N_2}^l \tag{55}$$

$$X(\bar{\omega}_h,\omega_l) = H\,Z(\bar{\omega}_h,\omega_l) \tag{56}$$

exactly coincide with equations (47)–(48) in (Soverini and Söderström, 2017) when the following substitutions are introduced

$$k = l \qquad N = N_2 \qquad A = F_2 \qquad C = H$$

$$Z(\omega_k) = Z(\bar{\omega}_h,\omega_l) \quad X(\omega_k) = X(\bar{\omega}_h,\omega_l) \quad T = \bar{T}_2(\bar{\omega}_h).$$

Introducing the notations $Z_l = Z(\bar{\omega}_h,\omega_l)$, $X_l = X(\bar{\omega}_h,\omega_l)$ and $B_2 = \bar{T}_2(\bar{\omega}_h)/\sqrt{N_2}$, the resulting model is

$$W_{N_2}^l\,Z_l = F_2\,Z_l + B_2\,W_{N_2}^l \tag{57}$$

$$X_l = H\,Z_l \tag{58}$$

which is analogue to (39)–(40). In this case the F–ESPRIT algorithm is applied to the rows of the matrix $\mathbf{X}$, obtaining the final relation

$$\mathbf{\Sigma} = \mathcal{O}_{(m+1)}\,\mathbf{P}\,\mathcal{O}_{(m+1)}^H. \tag{59}$$

Even if (59) formally coincides with (53), their terms are different since (53) refers to the t_1 axis, while (59) refers to the t_2 axis. In particular, the matrix $\mathcal{O}_{(m+1)}$ in (59) is the observability matrix with respect to F_2. As done before, starting from (59) it is then possible to implement the classical ESPRIT in order to recover the state–transition matrix F_2 and its eigenvalues.

5. NUMERICAL EXAMPLES

In this section, the effectiveness of the proposed procedure is tested by means of numerical simulations. The new method is compared with the 2D–TD–KUNG method (see Appendix A) and with the 2D–FD–ESPRIT–ENH method (Soverini and Söderström, 2018). It is shown that the 2D–F–ESPRIT and the

Table 2. True and estimated values of the parameters ω_{1i}, ω_{2i}, β_{1i} and β_{2i} – SNR=25 dB

	$2D-F-ESPRIT$				$2D-FD-ESPRIT-ENH$			
	ω_{1i}	ω_{2i}	β_{1i}	β_{2i}	ω_{1i}	ω_{2i}	β_{1i}	β_{2i}
$i=1$	0.2065 ± 0.0358	-0.0100 ± 0.0001	0.0637 ± 0.0462	0.0600 ± 0.0008	0.2070 ± 0.0387	-0.0100 ± 0.0001	0.0611 ± 0.0225	0.0600 ± 0.0008
$i=2$	-0.2268 ± 0.0126	0.1850 ± 0.0008	0.0713 ± 0.0118	0.0800 ± 0.0051	-0.2271 ± 0.0146	0.1850 ± 0.0008	0.0705 ± 0.0078	0.0800 ± 0.0051
$i=3$	-0.2102 ± 0.0021	0.1999 ± 0.0008	0.0701 ± 0.0038	0.0901 ± 0.0063	-0.2102 ± 0.0021	0.1999 ± 0.0011	0.0700 ± 0.0037	0.0899 ± 0.0023
$i=4$	0.0433 ± 0.0378	-0.0600 ± 0.0002	0.1375 ± 0.0498	0.0900 ± 0.0013	0.0423 ± 0.0388	-0.0600 ± 0.0002	0.1404 ± 0.0623	0.0900 ± 0.0063
$i=5$	0.0667 ± 0.0285	0.3200 ± 0.0005	0.1887 ± 0.0341	0.2896 ± 0.0026	0.0668 ± 0.0287	0.3200 ± 0.0005	0.1883 ± 0.0345	0.2896 ± 0.0025

2D–FD–ESPRIT–ENH algorithms have very similar behaviors and are both characterized by high frequency resolution properties.

Example 1. As first example, the same system already proposed in (Soverini and Söderström, 2018) has been considered. It mimics a Magnetic Resonance data analysis, constituted by a model of type (1)–(2) with $n = 5$ components. The true frequency and damping parameters are reported in Table 1, together with the complex gains (not estimated).

The number of samples of the considered data matrix is $N_1 = 200$, $N_2 = 200$ and the sampling frequency is $f_s = 1$ Hz, so that the frequency resolution results in $df = f_s/N = 0.005$ Hz.

A Monte Carlo simulation of 100 independent runs has been performed by adding to the noise–free sequences $x(t)$ different circular white noise realizations with variance $\sigma_v^* = 21.4364$, corresponding to a Signal to Noise Ratio (SNR) of 25 dB.

Table 2 reports the empirical means of the estimates of the system parameters ω_{1i}, ω_{2i}, β_{1i} and β_{2i}, together with the corresponding standard deviations, obtained with the proposed 2D–F–ESPRIT algorithm. The table reports also the results obtained with the 2D–FD–ESPRIT–ENH algorithm. For both methods the order $m > n$ of the augmented model has been fixed to $m = 66$. For the definition of m, see (42)–(43) for the 2D–F–ESPRIT method and (Soverini and Söderström, 2018) for the 2D–FD–ESPRIT–ENH algorithm. Table 2 shows that in this case both identification methods yield similar, very good results.

Example 2. The example considers the 2D NMR simulated system of type (1)–(2) with $n = 5$ components, proposed in (Li et al., 1998). The true frequency and damping parameters are reported in the first four columns of the Table 3. The complex gains are $\rho_i = 100\,\mathrm{e}^{0.5\pi}$ ($i = 1, \ldots, 5$).

The number of samples of the considered data matrix is $N_1 = 200$, $N_2 = 200$ and the sampling frequency is $f_s = 1$ Hz, so that the frequency resolution results in $df = f_s/N = 0.005$ Hz. The contour plot of the 2D–DFT spectrum is shown in Fig. 1.

Note that $\omega_{21} = \omega_{22}$. Thus, the model does not satisfies the assumption A2, requiring that the n frequencies are distinct in both directions. Strictly speaking, this identifiability condition concerns the case of pure sinusoids. The presence of damping parameters different from zero may lead to some identification advantages, as shown by the results obtained with the time domain 2D-TD-KUNG method (see table 4). For the two frequency domain algorithms, this drawback can be overcome by using the area–selective features.

A Monte Carlo simulation of 100 independent runs has been performed by adding to the noise–free sequences $x(t)$ different

Table 3. System parameters and sub–areas

	ω_{1i}	ω_{2i}	β_{1i}	β_{2i}	$W_1 \times W_2$
$i=1$	0.050	0.050	0.20	0.10	$[0.0,\ 0.1] \times [0.0,\ 0.1]$
$i=2$	0.150	0.050	0.00	0.00	$[0.1,\ 0.2] \times [0.0,\ 0.1]$
$i=3$	0.100	0.125	0.05	0.02	$[0.05,\ 0.15] \times [0.075,\ 0.175]$
$i=4$	0.025	0.150	0.02	0.02	$[0.0,\ 0.075] \times [0.125,\ 0.175]$
$i=5$	0.030	0.155	0.10	0.02	

circular white noise realizations with variance $\sigma_v^* = 152$, corresponding to a Signal to Noise Ratio (SNR) of 20 dB.

Table 4 reports the empirical means of the estimates of the system parameters ω_{1n} and ω_{2n}, together with the corresponding standard deviations, obtained with the proposed 2D–F–ESPRIT algorithm. The table reports also the results obtained with the time domain 2D–TD–KUNG algorithm and with the 2D–FD–ESPRIT–ENH algorithm. The 2D–TD–KUNG estimates simultaneously all the five frequencies along the t_1 and t_2 axis. On the contrary, the estimates of the 2D–F-ESPRIT and the 2D–FD–ESPRIT–ENH algorithms have been obtained by a proper selection of the 2D frequency sub–area $W_1 \times W_2$ of the spectrum. The last column of Table 3 reports the frequency sub–bands $W_1 \times W_2$ (in Hz) used for the identification of the n peaks. Both the frequency domain methods make use of the same sub–areas.

Table 4 shows that the 2D–F–ESPRIT and the 2D–FD–ESPRIT–ENH algorithms yield similar, good results. Two facts are worth observing. As already pointed out, the two algorithms cannot discriminate the frequencies $\omega_{21} = \omega_{22} = 0.050$ along the t_2 axis. Good estimates of the two peaks (ω_{11}, ω_{21}) and (ω_{12}, ω_{22}) have been obtained by using two disjoint sub–areas. Since the two peaks (ω_{14}, ω_{24}) and (ω_{15}, ω_{25}) are very close to each other, the same sub–area has been used for their joined estimates, in other words the number of 2D sinusoids to be identified in that area has been fixed to $n = 2$.

6. CONCLUSIONS

In this paper a novel 2D–frequency subspace–based approach has been proposed for the identification of complex sinusoids affected by additive white noise. Its estimation properties have been tested and compared by means of Monte Carlo simulations. The numerical results have confirmed the good performance of the new method.

Appendix A. 2D TIME DOMAIN SOLUTION

In the following, a revised version of the 2D time domain realization procedure proposed in (Kung et al., 1983) is described.

Table 4. Estimated values of the parameters ω_{1i} and ω_{2i} – SNR=20 dB

	$2D-TD-KUNG$		$2D-FD-ESPRIT-ENH$		$2D-F-ESPRIT$	
	ω_{1i}	ω_{2i}	ω_{1i}	ω_{2i}	ω_{1i}	ω_{2i}
$i=1$	0.1002 ± 0.0003	0.0489 ± 0.0003	0.0383 ± 0.0021	0.0477 ± 0.0023	0.0394 ± 0.0018	0.0477 ± 0.0020
$i=2$	0.1508 ± 0.0003	0.0570 ± 0.0020	$0.1500 \pm 4.5667 * 10^{-6}$	$0.0500 \pm 5.6463 * 10^{-6}$	$0.1500 \pm 5.1006 * 10^{-6}$	$0.0500 \pm 6.1058 * 10^{-6}$
$i=3$	0.1421 ± 0.0020	0.1253 ± 0.0001	$0.0997 \pm 5.0949 * 10^{-4}$	$0.1265 \pm 2.6291 * 10^{-4}$	$0.0996 \pm 5.1684 * 10^{-4}$	$0.1268 \pm 2.8250 * 10^{-4}$
$i=4$	0.0248 ± 0.0002	0.1492 ± 0.0004	0.0245 ± 0.0001	$0.1349 \pm 0.9453 * 10^{-3}$	0.0244 ± 0.0001	$0.1348 \pm 0.9073 * 10^{-3}$
$i=5$	0.0289 ± 0.0012	0.1514 ± 0.0007	0.0481 ± 0.0024	$0.1510 \pm 0.1146 * 10^{-3}$	0.0481 ± 0.0024	$0.1510 \pm 0.1108 * 10^{-3}$

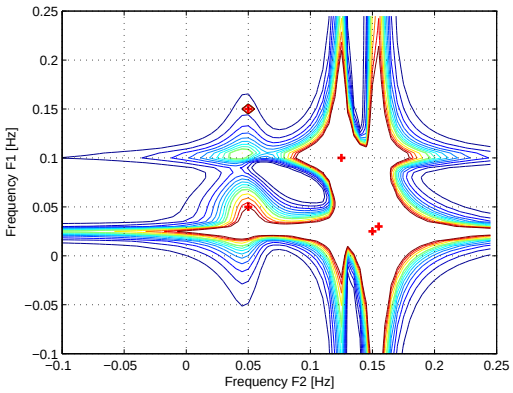

Fig. 1. Contour plot of the 2D–DFT spectrum.

Consider the 2D state–space representation (3)–(5) and collect the noise–free output data $x(t_1, t_2)$ in the matrix

$$X = \begin{bmatrix} x(0,0) & x(0,1) & \dots & x(0,N_2-1) \\ x(1,0) & x(1,1) & \dots & x(1,N_2-1) \\ \vdots & \vdots & \ddots & \vdots \\ x(N_1-1,0) & x(N_1-1,1) & \dots & x(N_1-1,N_2-1) \end{bmatrix}. \tag{A.1}$$

The matrix X has finite rank n and is factorizable as follows

$$X = \mathcal{O}_1 \, \Gamma, \tag{A.2}$$

where

$$\mathcal{O}_1 = \begin{bmatrix} H \\ HF_1 \\ HF_1^2 \\ \vdots \\ HF_1^{N_1-1} \end{bmatrix} \tag{A.3}$$

$$\Gamma = \left[x(0,0),\ F_2\, x(0,0),\ F_2^2\, x(0,0),\ \dots,\ F_2^{N_2-1}\, x(0,0) \right]. \tag{A.4}$$

If the covariances are defined as the following temporal average

$$r(h,l) = \lim_{\substack{N_1\to\infty \\ N_2\to\infty}} \frac{1}{N_1 N_2} \sum_{t_1=0}^{N_1-1} \sum_{t_2=0}^{N_2-1} x(t_1+h, t_2+l) x^*(t_1,t_2), \tag{A.5}$$

then it is easily seen using (3)–(5) that the covariance $r(h,l)$ satisfies the relation

$$r(h,l) = H\, F_1^h\, F_2^l\, P\, H^T, \tag{A.6}$$

where P is the state covariance matrix

$$P = \lim_{\substack{N_1\to\infty \\ N_2\to\infty}} \frac{1}{N_1 N_2} \sum_{t_1=0}^{N_1-1} \sum_{t_2=0}^{N_2-1} z(t_1,t_2) z^H(t_1,t_2). \tag{A.7}$$

Collecting the elements $r(h,l)$ in the following covariance matrix

$$R = \begin{bmatrix} r(0,0) & x(0,1) & \dots & x(0,N_2-1) \\ x(1,0) & x(1,1) & \dots & x(1,N_2-1) \\ \vdots & \vdots & \ddots & \vdots \\ x(N_1-1,0) & x(N_1-1,1) & \dots & x(N_1-1,N_2-1) \end{bmatrix}, \tag{A.8}$$

it is possible to prove that R is factorizable as follows

$$R = \mathcal{O}_1 \, {\mathcal{O}_2}^T, \tag{A.9}$$

where $\mathcal{O}_1$ has been defined in (A.3) and

$$\mathcal{O}_2 = \begin{bmatrix} H\, P^T \\ H\, P^T F_2^T \\ H\, P^T {F_2^T}^2 \\ \vdots, \\ H\, P^T {F_2^T}^{N_2-1} \end{bmatrix}. \tag{A.10}$$

Thus, also matrix R has finite rank n. Let

$$\mathcal{O}_1\uparrow = [\, I_{N_1}\ 0\,]\, \mathcal{O}_1 \tag{A.11}$$

$$\mathcal{O}_1\downarrow = [\, 0\ I_{N_1}\,]\, \mathcal{O}_1, \tag{A.12}$$

where I_{N_1} is the identity matrix of dimension $N_1 \times N_1$. Note that $\mathcal{O}_1\uparrow$ ($\mathcal{O}_1\downarrow$) is obtained from $\mathcal{O}_1$ by deleting the last (first) row. Clearly,

$$\mathcal{O}_1\downarrow = \mathcal{O}_1\uparrow\, F_1. \tag{A.13}$$

Analogously, let

$$\mathcal{O}_2\uparrow = [\, I_{N_1}\ 0\,]\, \mathcal{O}_2 \tag{A.14}$$

$$\mathcal{O}_2\downarrow = [\, 0\ I_{N_1}\,]\, \mathcal{O}_2, \tag{A.15}$$

where I_{N_2} is the identity matrix of dimension $N_2 \times N_2$. It results in

$$\mathcal{O}_2\downarrow = \mathcal{O}_2\uparrow\, F_2^T. \tag{A.16}$$

The relations (A.13) and (A.16) allow to develop classical subspace–based algorithms for the determination of the eigenvalues of the matrices F_1 and F_2.

For this purpose, one can use the well–known ESPRIT algorithm (Roy and Kailath, 1989). According to the partition (A.9)–(A.10), when the method is applied to the matrix R in (A.8), it determines the eigenvalues $\lambda_{1i} = \mathrm{e}^{\gamma_{1i}}$ of F_1 ($i = 1, \dots, n$). When the method is applied to R^T, it determines the eigenvalues $\lambda_{2i} = \mathrm{e}^{\gamma_{2i}}$ of F_2 ($i = 1, \dots, n$).

For example, making reference to R and $\mathcal{O}_1$, the eigenvalues of F_1 can be determined as follows. Select an integer $m > n_1$ (user choice) and construct the matrix R of type (A.8), with dimension $(m+1) \times (m+1)$. Note that R, in general, is complex and not symmetric. Then, compute the singular value decomposition

$$R = U\, \Sigma\, V^H \tag{A.17}$$

and proceed with the classical ESPRIT algorithm. See, for example, Section 5 in (Soverini and Söderström, 2017).

Analogous considerations hold for R^T and $\mathcal{O}_2$, for the determination of the eigenvalues of F_2.

Appendix B. IDENTIFICATION OF THE GAINS ρ

In this appendix the 2D–frequency domain pairing procedure described in (Sandgren et al., 2006) is briefly recalled.

Starting from the estimates of the parameters $\gamma_{1i} = -\beta_{1i} + \mathrm{i}\omega_{1i}$ and $\gamma_{2i} = -\beta_{2i} + \mathrm{i}\omega_{2i}$, the procedure determines the correct pairs $\{\gamma_{1i}, \gamma_{2i}\}_{i=1}^{n}$ and computes the estimates of the complex gains $\{\rho_i\}_{i=1}^{n}$, in order to recover the original signal (1).

These two operation can be performed simultaneously in the 2D frequency domain, by minimizing the sum of the squared errors between the original data and the reconstructed noise–free data, with respect to $\{\rho_i\}_{i=1}^{n}$. This minimization has to be performed for all possible pairs $\{\gamma_{1i}, \gamma_{2i}\}_{i=1}^{n}$.

When the whole data set is considered, the minimization problem can be written as

$$\min_{\{\rho_i\}} \sum_{h=0}^{N_1-1} \sum_{l=0}^{N_2-1} |Y(\omega_h, \omega_l) - \sum_{i=1}^{n} \rho_i C_i(\omega_h, \omega_l)|^2 \qquad \text{(B.1)}$$

where C_i is defined as the 2D–DFT of the reconstructed data for the i–th component, based on a specific pairing combination $\{\gamma_{1i}, \gamma_{2i}\}_{i=1}^{n}$

$$C_i(\omega_h, \omega_l) = \frac{1}{\sqrt{N_1 N_2}} \sum_{t_1=0}^{N_1-1} \sum_{t_2=0}^{N_2-1} \mathrm{e}^{\gamma_{1i}\, t_1}\, \mathrm{e}^{\gamma_{2i}\, t_2}\, \mathrm{e}^{-\mathrm{i}\omega_h t_1}\, \mathrm{e}^{-\mathrm{i}\omega_l t_2} \qquad \text{(B.2)}$$

where $\omega_h = 2\pi h/N_1$ ($h = 0, \ldots, N_1 - 1$) and $\omega_l = 2\pi l/N_2$ ($l = 0, \ldots, N_2 - 1$).

Define with $\mathbf{c}_i(l)$ and with $\mathbf{y}(l)$ the l–th columns of the matrices $\mathbf{C}_i$ and $\mathbf{Y}$, whose elements are $\{C_i(\omega_h, \omega_l)\}$ and $\{Y(\omega_h, \omega_l)\}$.

The solution to (B.1) can be obtained as

$$\rho = \begin{bmatrix} \rho_1 \\ \rho_2 \\ \vdots \\ \rho_n \end{bmatrix} = \sum_{l=0}^{N_2-1} \left(\begin{bmatrix} \mathbf{c}_1^*(l) \\ \mathbf{c}_2^*(l) \\ \vdots \\ \mathbf{c}_n^*(l) \end{bmatrix} [\mathbf{c}_1(l)\ \mathbf{c}_2(l)\ \ldots\ \mathbf{c}_n(l)] \right)^{-1}$$
$$\times \sum_{l=0}^{N_2-1} \left(\begin{bmatrix} \mathbf{c}_1^*(l) \\ \mathbf{c}_2^*(l) \\ \vdots \\ \mathbf{c}_n^*(l) \end{bmatrix} [\mathbf{y}(l)\ \mathbf{y}(l)\ \ldots\ \mathbf{y}(l)] \right). \qquad \text{(B.3)}$$

The pairing procedures is completed by selecting the combination $\{\gamma_{1i}, \gamma_{2i}\}_{i=1}^{n}$ which gives the smallest sum of the squared errors in (B.1).

REFERENCES

Clark, M.P. and Sharf, L.L. (1994). Two–dimensional modal analysis based on maximum likelihood. *IEEE Transactions on Signal Processing*, 42(6), 1443–1452.

Gunnarsson, J. and McKelvey, T. (2007). Reducing noise sensitivity in F-ESPRIT using weighting matrices. *EUSIPCO 2007*, Poznan, Poland, 783–787.

Hua, Y. (1992). Estimating two–dimensional frequencies by matrix enhancement and matrix pencil. *IEEE Transactions on Signal Processing*, 40, 2267–2280.

Hua, Y. and Baqai, F. (1994). Correction to: Estimating two–dimensional frequencies by matrix enhancement and matrix pencil. *IEEE Transactions on Signal Processing*, 42, 1288.

Kung, S.Y., Arun, K.S. and Bhaskar Rao, D.V. (1983). State–space and singular value decomposition–based approximation methods for harmonic retrieval problem. *Journal of Optical Society of America*, 73(12), 1799–1811.

Li, Y., Razavilar, J. and Ray Liu, K.J. (1998). A high–resolution technique for multidimensional NMR spectroscopy. *IEEE Transactions on Biomedical Engineering*, 45, 78–86.

Li, J., Stoica, P. and Zheng, D. (1996). An efficient algorithm for two–dimensional frequency estimation. *Multidimensional Systems and Signal Processing*, 7, 151–178.

Marple, L. (2000). Two–dimensional lattice linear prediction parameter estimation method and fast algorithm. *IEEE Signal Processing Letters*, 7(6), 164–168.

McKelvey, T. (2000). Frequency domain identification. *Proc. of the 12th IFAC Symposium on System Identification*, Plenary Paper. Santa Barbara, California USA.

McKelvey, T. (2002). Frequency domain identification methods. *Circuits Systems Signal Processing*, 21(1), 39–55.

McKelvey, T. and Viberg, M. (2001). A robust frequency domain subspace algorithm for multi–component harmonic retrieval. *Proc. of the 35th Asilomar Conference on Signals, Systems and Computers*, Pacific Grove, CA, 1288–1292.

Pintelon, R. and Schoukens, J. (2012). *System identification: a frequency domain approach* (2nd ed.). NY: IEEE Press.

Pintelon, R., Schoukens, J. and Vandersteen G. (1997). Frequency domain system identification using arbitrary signals. *IEEE Transactions on Automatic Control*, 42, 1717–1720.

Roesser, R.P. (1975). A discrete state-space model for linear image processing. *IEEE Trans. on Automatic Control*, 20(1), 1–10.

Rouquette, S. and Najim, M. (2001). Estimation of frequencies and damping factors by two–dimensional ESPRIT methods. *IEEE Transactions on Signal Processing*, 49, 237–245.

Roy, R. and Kailath, T. (1989). ESPRIT–Estimation of signal parameters via rotational invariance techniques. *IEEE Transactions on Acoustics, Speech and Signal Processing*, 37, 984–995.

Sandgren, N., Stoica, P. and Frigo, F.J. (2006). Area–selective signal parameter estimation for two–dimensional MR spectroscopy data. *Journal of Magnetic Resonance*, 183, 50–59.

Sacchini, J.J., Steedy, W.M. and Moses, R.L. (1993). Two–dimensional Prony modeling and parameter estimation. *IEEE Transactions on Signal Processing*, 41, 3127–3136.

Soverini, U. and Söderström, T. (2017). Frequency domain identification of complex sinusoids in the presence of additive noise. *Proc. of the 20–th IFAC World Conference*, Toulouse, France, 6418–6424.

Soverini, U. and Söderström, T. (2018). 2D-frequency domain identification of complex sinusoids in the presence of additive noise. Accepted for presentation at the *18–th IFAC SYSID*, Stockholm, Sweden.

Stoica, P. and Moses, R. (1997). *Introduction to Spectral Analysis*, Prentice–Hall, Upper Saddle River, New Jersey, 1997.

Vanpoucke, F., M.Moonen, Y. and Berthoumieu, Y. (1994). An efficient subspace algorithm for 2–D harmonic retrieval. *Proc. of ICASSP*, Adelaide, Australia, 461–464.

Wang, Y., Chen J.W. and Liu, Z. (2005). Comments on: Estimation of frequencies and damping factors by two–dimensional ESPRIT methods. *IEEE Trans. on Signal Processing*, 53.

Zhu, Y. and Hua, Y. (1993). Spectral estimation of two–dimensional NMR signals by matrix pencil method. *Proc. Comp. Commun. Control Power Eng*, 3, 546–549.